

Itraconazole Loaded Micelle Based on Methoxy Poly(Ethylene Glycol)-Poly(D, L-Lactic Acid) for Ocular Drug Delivery: In vitro and in vivo Evaluation

Jijun He*, Jingjing Yang*, Zhen Liang, Zhen Zhang, Guojuan Pu, Fudan Dong, Ping Lu, Huiyun Xia, Junjie Zhang

Henan Eye Hospital, Henan Provincial People's Hospital, Zhengzhou University People's Hospital, Zhengzhou, People's Republic of China

*These authors contributed equally to this work

Correspondence: Junjie Zhang, Email zhangjunjie@zzu.edu.cn

Purpose: This study aimed to develop itraconazole (ITZ)-loaded polymer micelles using methoxy poly(ethylene glycol)-poly(D, L-lactic acid) (mPEG-PDLLA) as a carrier to improve the ocular bioavailability of ITZ after topical administration.

Methods: ITZ-loaded mPEG-PDLLA micelles (ITZ-M) were prepared using the thin-film dispersion method and were characterized by droplet size (DS), zeta potential (ZP), polydispersity index (PDI), morphology, entrapment efficiency (EE%), and critical micelle concentration (CMC). In vitro drug release from ITZ-M, the storage stability and cytotoxicity in human corneal epithelial cells (HCECs) were studied. In vivo transcorneal permeation of micelles labeled with coumarin 6 (C6) was observed using two-photon confocal microscopy, in vivo ocular irritation and pharmacokinetics in rabbit eyes were investigated.

Results: The ITZ-Ms were uniform spherical particles with DS of 18.79 ± 0.16 nm and narrow distribution (PDI of 0.037 ± 0.019), the EE% was nearly 100%, and the CMC of the micelles was 0.083mM. Approximately 60% of the drug was released from the ITZ-M within 72 h, which was significantly higher than that released from the ITZ suspension. The results of the stability study and cytotoxicity assays demonstrated that ITZ-M possessed good physical stability at 4°C and have no toxicity to HCECs. Transcorneal studies indicated that the fluorescence intensity (FI) was mostly enriched in the corneal epithelium, which was reduced in the stroma. The FI in the epithelium and stroma for C6 micelles was much stronger than that in the C6 suspension. Ocular irritation evaluation revealed that ITZ-M was well tolerated. Ocular pharmacokinetic analysis indicated that the area under the curve (AUC_{0-240min}) values in the cornea and conjunctiva of rabbit eyes treated with ITZ-M were approximately 410.9- and 2.3-fold higher, respectively, than those treated with ITZ suspension.

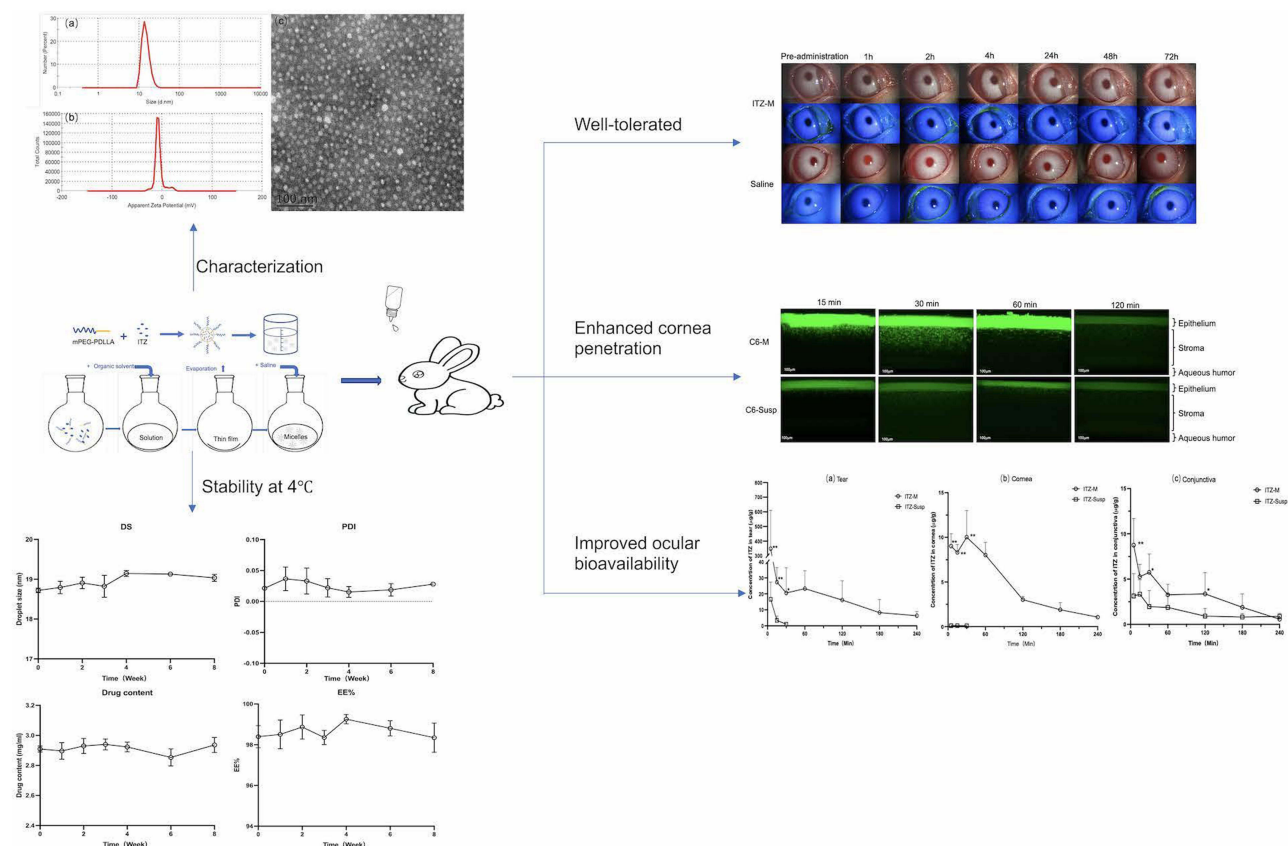
Conclusion: This study provides a potential formulation of ITZ for the treatment of fungal keratitis with good tolerability and improved ocular bioavailability.

Keywords: fungal keratitis, itraconazole, methoxy poly(ethylene glycol)-poly(D,L-lactic acid), polymeric micelle, ocular pharmacokinetic

Introduction

Fungal keratitis (FK) is a serious sight-threatening disease that can lead to permanent blindness and even lose eyeball.¹ It has been reported that the incidence of FK varies in most reports from 17% to 36% of cases with corneal infection.² In the United States, FK was reported to account for 5–20% of corneal infections, but the incidence was much higher in developing countries in tropical and subtropical regions, and it was reported to account for more than 50% of the total culture-positive microbial keratitis cases.³ It requires prompt and effective treatment. Lack of proper treatment can cause corneal destruction and endophthalmitis, leading to vision loss, and early diagnosis and treatment are crucial to prevent

Graphical Abstract



long-term complications and blindness.^{4,5} FK treatment involves two methods: drug and surgical treatment. Initially, less severe corneal infections may not demand aggressive management and can be intervened with topical antifungals administered at appropriate frequency, surgical management may be necessary in progressive resistant cases or for the management of complications.^{6–8} Antifungal medication is considered the main treatment for FK, and topical drug delivery remains the preferred route.⁹ Natamycin, approved by the Food and Drug Administration, is the only available commercially as an ocular preparation in a suspension form. Although natamycin has good activity against *Aspergillus* and is the first choice for *Fusarium*, its use has been limited due to its low efficacy against *Candida species* and poor corneal penetration.³ Hence, there is an urgent need to develop appropriate antifungal agents for topical and ocular use.

Itraconazole (ITZ), a triazole antifungal agent, is active against a broad spectrum of fungal species including *Cryptococcus*, *Candida*, *Aspergillus*, *Blastomyces* et al.¹⁰ The action mechanism of ITZ is related to its binding of fungal cytochrome P-450 with resultant inhibition of ergosterol synthesis and perturbation of membrane-bound enzyme function and membrane permeability.¹¹ ITZ is a highly lipophilic compound with $\log P$ of 5.7 and has very poor ionization ($pK_a = 3.7$) and solubility (about 4 ng/mL).^{12,13} Attempts have been made to instill ITZ to the eye topically. Rajasekaran et al reported that the administration of 1% ITZ cream to the eye was effective in less serious FK.¹⁴ Another study also reported that 1% ITZ suspension, which was prepared in a commercial isotonic eye drop formulation, was well tolerated when used for curing FK; however, it was not very effective in treating severe FK, perhaps due to insufficient corneal penetration.¹⁵ ITZ (2.5 mg/mL, with polyethylene glycol 200 as a solubilizer) could persist for at least 24 h in normal and debrided corneas after subconjunctival administration, compared to amphotericin B, miconazole, fluconazole, and ketoconazole, which did not maintain over 4–8 h.¹⁶ Therefore, it is necessary to formulate an ITZ ocular drug delivery system that could improve its therapeutic effects after topical administration.

It is difficult for many antifungal agents to penetrate the cornea effectively. Lipophilic compounds, such as ITZ, could easily cross the lipid-rich epithelial and endothelial cell membranes and the blood-aqueous barrier; hydrophilic compounds more easily cross the corneal stroma, and biphasic compounds, which possess both the lipid and water solubility, penetrate all corneal layers.¹⁷ Due to its poor water solubility, ITZ has low corneal penetration, which leads to low ocular bioavailability. Various novel nanoscale carriers have been introduced to enhance intraocular penetration and ocular bioavailability of poor corneal permeable drugs, such as liposomes, nanoemulsions, micelles and nanoparticles.^{18–20} Micellar solubilization have always gained considerable attention because of the polymer carriers, which have unique core-shell structure and high drug-loading capacity for enhancing the bioavailability of the poorly soluble drugs.²¹ Recently, self-assembled polymer micelles with amphiphilic blocks, as drug delivery system, represent a series of nanocarriers with a well-defined core-shell structure, they can overcome the poor water solubility of antifungal drugs and enhance the drugs' delivery to target sites through passive or active targeting.^{22–24} Moreover, polymeric micelles are biocompatible, biodegradable, non-toxic and exhibit improvement in bioavailability at the target site.^{25,26} Methoxy poly (ethylene glycol)-poly(D, L-lactic acid) (mPEG-PDLLA) is a self-assembled copolymer with a hydrophilic shell (PEG) and a hydrophobic core (PDLLA), it is biodegradable and exhibits good biocompatibility with PEG and PDLLA polymers as its components, both of which have been recognized and listed as safe by FDA.²⁷ In addition, mPEG-PDLLA has been shown that it could increase the solubility of the drug, allows controlled and sustained release of the drug and maintains better bioactivity of the drug.^{21,28,29}

The purpose of this study was to develop ITZ-loaded mPEG-PDLLA micelles (ITZ-M) as ocular drug delivery systems for FK treatment. The physical and chemical properties of the micelles included the droplet size (DS), polydispersity index (PDI), zeta potential (ZP) and entrapment efficiency (EE). The critical micelle concentration (CMC) and in vitro drug release kinetics of the micelles were investigated, and toxicity to human corneal epithelial cells (HCECs) was assayed. Ocular irritation and pharmacokinetics were evaluated in the rabbit eyes.

Materials and Methods

Materials

ITZ was purchased from Macklin Biochemical Co., Ltd. (Shanghai, China), and mPEG₂₀₀₀-PDLLA₂₀₀₀ was purchased from Daigang Biotech. Co., Ltd. (Jinan, China). High-performance liquid chromatography (HPLC) grade methanol and acetonitrile were purchased from Merck (Darmstadt, Germany) and Tedia Company Inc. (OH, USA), respectively. All other reagents were of analytical grade.

HCECs (ATCC CRL-11135) were cultured in Dulbecco's Modified Eagle's medium (DMEM) supplemented with 10% (v/v) fetal bovine serum and 1% (v/v) dual antibody. All the cells were maintained at 37°C incubator in a humidified 5% CO₂ atmosphere. The culture plates and dishes were purchased from Corning (Corning, NY, USA).

New Zealand white rabbits (each weighing 2.0–2.5 kg) used in the ocular irritation and pharmacokinetics studies were provided by Huaxing Experiment Animal Breeding Co. (Zhengzhou, China). The animals were kept in an air-conditioned and light controlled room at a temperature of 20 ± 5°C and relative humidity of 60 ± 5%, the rabbits were provided with a standard diet and free access to drinking water. All animal protocols were approved by the Ethical Committee of Experimental Animal Care of the Henan Eye Institute (approval no. HNEECA-2022-32) and conducted in accordance with the guidelines of the National Institutes of Health and the Association for Research in Vision and Ophthalmology Resolution.

Preparation of ITZ-M

The thin-film dispersion method was used to prepare ITZ-M. Briefly, ITZ (30 mg) and mPEG-PDLLA (1.5 g) was dissolved in 20 mL of organic solvent (methanol:acetonitrile = 1:1, v:v) to form a clear solution. The solvent was completely evaporated using a rotary evaporator under vacuum at 60°C to obtain a thin membrane on the round-bottom flask wall. Then the ITZ-M was prepared after the thin membrane was hydrated with 10 mL of phosphate buffer saline solution (PBS, pH 7.0) at 60°C for 10 min. The formed ITZ-M was filtered through a 0.22-μm Millipore filtration membrane to remove impurities. A blank micelle solution was prepared using the same method.

The ITZ suspension (ITZ-Susp) was prepared by dissolving an equal amount of drug in PBS, which contained 1% Tween 80 and 0.2% sodium carboxymethyl cellulose, and was pulverized using probe ultrasound to make the particle size smaller than 10 μm , which could be used as a control in the in vitro drug release study and in vivo ocular pharmacokinetics study.

Fluorescein labeled micelles were prepared and used for transcorneal penetration in vivo. Coumarin 6 (C6, 5 mg) and mPEG-PDLLA (1.5 g) were co-dissolved in 20 mL of organic solvent (methanol:acetonitrile = 1:1, v:v) to form a diaphanous clear solution, the followed fabrication process is the same as the preparation of ITZ-M. C6 loaded micelles (C6-M) were purified using ultrafilter with MWCO of 3000 Da (Amicon Ultra, Merck Millipore Ltd., Ireland) to remove the free C6.

Analytical Methods

ITZ was determined quantitatively through high performance liquid chromatography (HPLC)-UV method according to previous report,³⁰ the conditions were minorly modified to be more suitable and the assay method was validated by specificity, sensitivity, and stability linearity, recovery, precision and accuracy and stability. Briefly, HPLC system (2695, Waters, MA, United States) equipped with ultraviolet detection (2487, Waters, MA, United States) was used, an X-Bridge C18 column (3.5 μm , 3.0 \times 150 mm) was used at a temperature of 40°C. The mobile phase consisted of acetonitrile and water (40:60, v/v) at a flow rate of 0.5 mL/min, the detection wavelength was set at 262 nm. The injection volume was 20 μL and the limit of quantitation of ITZ for this method was approximately 0.02 $\mu\text{g/mL}$, which was used to determine the drug content of the micelles, stability, and in vivo ocular pharmacokinetics.

Particle Size and Zeta Potential

The DS, PDI, and ZP of the micelles were measured by the dynamic light scattering method using a Zetasizer (Nano ZS90, Malvern Instruments, United Kingdom). The light scattering was monitored at 25°C at an angle of 90° after the sample was appropriately diluted with purified water. Each sample was analyzed in triplicate.

Morphology

Morphological observations of ITZ-M were performed by transmission electron microscopy (TEM) (Joel JEM 1230, Tokyo, Japan). Briefly, a drop of micelle solution was loaded onto a copper grid. The excess solution was removed using filter paper. The micelles were negatively stained with phosphotungstic acid solution (2%, w/v) and loaded into the TEM system for observation after the carbon grid was air-dried at room temperature.

Entrapment Efficiency

The EE% of ITZ in the micelles was measured using the ultrafiltration method. To separate free drugs from the ITZ-M in the aqueous phase, 4 mL of the micelles was added to the upper cells of the ultrafiltration tube with an MWCO of 3000 Da (Amicon Ultra, Merck Millipore Ltd. Ireland), and centrifuged (5810R, Eppendorf, Germany) at 4000 rpm for 10 min. The filtrate was diluted with acetonitrile for HPLC analysis. The EE% was calculated as follows:

$$\text{EE\%} = (W_t - W_f) / W_t \times 100 \quad (1)$$

where W_t is the total mass of the ITZ in the micelles and W_f is the free mass of ITZ in the aqueous phase.

Critical Micelle Concentration (CMC)

The CMC of mPEG-PDLLA was determined using the surface tension method.³¹ Briefly, a series of mPEG-PDLLA solution at different concentrations (0.0125–0.5 mM) were prepared. The surface tensions of the solutions were determined using a drop-shape analyzer (KRussDSA25, DKSH, China). The surface tension was plotted against the polymer concentration, and the CMC values corresponded to the concentration of the polymer, where sharp decreases in surface tension were observed. The CMC value was obtained from the intersection point of the two lines and was established to describe the two linear parts of the plots under linear regression.

In vitro Drug Release Studies

The amount of ITZ released from ITZ-M was studied using the dialysis bag diffusion method in a constant temperature oscillator (Putian Instrument Co. Ltd., Changzhou City, Jiangsu Province, China) at 100 rpm and 35°C. 0.3 mL of each sample was sealed in a dialysis bag (MWCO of 3500 Da) and then placed into the release medium (200 mL), the artificial tear solution containing 2% (w/v) sodium dodecyl sulfate (pH 7.4). Five milliliters of each aliquot of the release medium were removed at predetermined time points, and an equal volume of release medium was replenished. ITZ-Susp served as a control, and the experiments were performed in triplicate. The amount of ITZ released was determined using a UV spectrophotometer (UV2000, Macy, Shanghai, China) at a wavelength of 262 nm. The cumulative amount of ITZ released was calculated using Equation (2).

$$Q(\%) = \frac{C_n V + V_i \sum_{i=0}^{i=n} C_i}{W_0} \times 100\% \quad (2)$$

Where W_0 is the initial amount of ITZ in the dialysis bag, C_n is the determined concentration of ITZ in the release medium at the prearranged n time point, V is 200 mL (eg, the volume of the release medium), V_i is 5 mL (eg, the sampling volume at time point i), and C_i is the determined concentration of ITZ in the sample at time point i.

The release kinetics and mechanism of ITZ from the micelles were fitted to different mathematical models, including zero-order, first-order, Higuchi, and Ritger-Peppas models, to assess the best kinetic model using the data obtained from the above tests.

Storage Stability

Storage stability of the ITZ-M were also evaluated, five milliliters of the ITZ-M solution were sealed into transparent glass bottles and placed under the conditions of 4°C and 25°C. The physical and chemical properties, including drug content, DS, PDI, and EE%, were determined after 1, 2, 3, 4, 6, and 8 weeks.

Cytotoxicity

The cytotoxicity of ITZ-M to HCECs was assayed using a cell counting kit-8 (CCK-8) assay. HCECs suspensions (100 μ L) were seeded in 96-well plates at a density of 1×10^4 cells/well and incubated for 24 h, after which the medium was removed. 100 μ L of the ITZ-M solution at drug concentrations of 1.5, 0.3, 0.06 and 0.03 mg/mL, which were diluted in growth medium, were added, and the wells containing cells were used as the control group and those without cells were used as the blank group. The cytotoxicity of mPEG-PDLLA micelles without ITZ (control group) after dilution was assayed using the same method. After culturing for 15 min, 1, 2 and 4h, respectively, the cells were washed with sterilized PBS, and 100 μ L of CCK-8 solution, diluted to 10% (v/v) with growth medium, was added to each well and incubated for another 3 h. The optical density (OD) of each well was measured at 450 nm using a microplate reader (Multiskan FC, Thermo Scientific, Shanghai, China) at a wavelength of 450 nm, and cell viability was calculated using the following equation:

$$\text{Cell viability}\% = \frac{OD_t - OD_b}{OD_c - OD_b} \times 100\% \quad (3)$$

where, OD_t , OD_b and OD_c are the absorption of the test, blank, and control groups, respectively.

In vitro Antifungal Activity

The agar plate diffusion method was used to test antifungal activity against *Aspergillus*. Briefly, four wells with a diameter of 6 mm were punched onto the agar plate using a cornea ring-drill, and 50 μ L of ITZ-M, ITZ-Susp, blank micelles, and voriconazole solution were added to each well after dilution to the appropriate concentrations with saline. Blank micelles and voriconazole solution served as the negative and positive controls, respectively. Each well contained 10 μ g ITZ, and the positive control well contained 5 μ g voriconazole. The inoculated plates were placed in an incubator at 37°C to culture for 24 h, the diameters of the inhibition zones were determined using a caliper.

In vivo Corneal Permeation Studies in Rabbit Eyes

The in vivo corneal permeation of the mPEG-PDLLA micelles in rabbit eyes was observed using an LSM 780 NLO two-photon laser scanning fluorescence microscope system (Carl Zeiss, Jena, Germany).³¹ In order to visually observe the transcorneal permeability of the micelles, the ITZ in the drug loaded micelles was replaced with C6. The C6 suspension (C6-Susp) was prepared using the same method as that used for the ITZ-Susp. 50 μ L of C6-M solution and C6-Susp were topically administered to the right and left eyes of four rabbits, respectively. The animals were sacrificed by intravenous administration of excess sodium phenobarbital at scheduled time points (15, 30, 60, and 120 min) after administration, and the eyeballs were enucleated for imaging, all of which were imaged within 30 min after enucleation. The eyeballs were held upward in a plastic holder, and the central region of the cornea was scanned using a 10- μ m z-axis step size to generate 3D images. The excitation and emission wavelengths were set at 700 nm and 500–550 nm, respectively.

Ocular Irritation Studies

ITZ-M irritation was assessed in rabbit eyes according to modified scoring criteria for ocular irritation using the Draize test. ITZ-M (100 μ L) was instilled into the right eyes of three rabbits without eye diseases, and the animals were administered five times continuously, at five minutes interval. The same amount of saline was instilled into the left eye to serve as a control. Any signs of damage to the eyelids, cornea, iris, and conjunctiva of both eyes were observed using an anterior segment camera system (Kanghua Ruiming, Chongqing, China) and scored according to the scoring criteria at 1, 2, 4, 24, 48, and 72 h after administration. Damage to the corneal epithelial layer was observed after a drop of fluorescein sodium solution was instilled under cobalt blue light.

The effects of ITZ-M on eyeball tissue were also evaluated. The eyeballs were enucleated and fixed in FAS eyeball fixative solution (Wuhan Servicebio Technology Co., Ltd., Wuhan, China) for 72h after sacrifice by injecting an overdose of sodium phenobarbital into the marginal ear vein. Sections (5 μ m thick) were cut and stained with hematoxylin and eosin (H&E), and tissue alterations were observed using a panoramic diagnostic scanner (Panoramic MIDI, 3D Histech, Hungary).

Ocular Pharmacokinetic Studies in Rabbit Eyes

Forty-two rabbits were randomly divided into experimental and control groups, with twenty-one animals in each group. Both eyes of animals in the experimental group were administered ITZ-M five times (50 μ L each time, at five minutes interval), and animals in the control group were administered ITZ-Susp. The animals were sacrificed by intravenous administration of an overdose of sodium phenobarbital at scheduled time points. The aqueous humor (AH) was drawn using a disposable sterile syringe from the limbus after the ocular surface of the eye was rinsed with saline and then precisely divided into aliquots of 100 μ L. The cornea and conjunctiva were collected, blotted up using filter paper, weighed accurately, then all samples were stored at -80°C until quantitative analysis.

The bioanalytical methods for the quantification of ITZ in tissues were validated for specificity, sensitivity, linearity, recovery, precision, accuracy, and stability and could be applied to assay the levels of drug in the tissue samples for pharmacokinetic studies. For HPLC analysis, the corneal and conjunctival samples were cut into pieces, immersed in 400 μ L of acetonitrile, all samples were placed at 4°C for 24 h. The aqueous solution (100 μ L) was mixed with 100 μ L acetonitrile and vortexed for 1 min. The processed corneal and aqueous samples were centrifuged (MiniSpin Plus, Eppendorf, Germany) at 12000 rpm for 10 min, and the supernatants were collected for HPLC analysis, as described above.

Statistical Analysis

All experimental data were expressed as mean \pm standard deviation (SD). The independent sample *t*-test was applied to compare the differences between the ITZ-M and ITZ-Susp with SPSS 26.0, and $p < 0.05$, which was considered statistically significant. Pharmacokinetic parameters were calculated using DAS 2.1 software (Anhui Provincial Center for Drug Clinical Evaluation, Wuhu, China).

Results and Discussion

Preparation and Characterization of ITZ-M

The molecular weight of the mPEG-PDLLA polymer used in this study was approximately 4000 Da and that of mPEG and PDLLA was 2000 Da. ITZ-M was prepared using the thin-film hydration method, in which the drug and polymer were distributed in an amorphous state during the evaporation of the organic solvent. The mPEG-PDLLA polymer assembled into core-shell structured micelles with ITZ encapsulated in the core after adding the PBS solution.

The EE% of ITZ-M was nearly 100%, suggesting that mPEG-PDLLA has a high encapsulation efficiency as a micelle carrier. Moreover, the DS of the ITZ-M was about 18.79 ± 0.16 nm (Figure 1a), the ZP was close to neutral (Figure 1b), the PDI was about 0.037 ± 0.019 , indicating that there was a narrow size distribution. According to the TEM micrograph (Figure 1c), ITZ-M had a spherical shape with smooth uniform surfaces, and no aggregates were observed, indicating that ITZ-M was physically stable. The DS was consistent with the results previously obtained using a Zetasizer.

CMC

The CMC of mPEG-PDLLA was determined using the surface-tension method. Figure 2 showed the surface tension versus the concentrations of mPEG-PDLLA, it could be obtained that the CMC value of the mPEG-PDLLA was about 0.083mM (Figure 2). Amphiphilic block copolymers can form micelles in the aqueous phase, and CMC, the physical parameter of micelles, indicates the thermodynamic stability of the micelles, a low CMC value ensures that the polymers self-assemble into stable micelles.

In vitro Drug Release and Kinetics

Figure 3 showed the in vitro release behavior of ITZ from ITZ-M and ITZ-Susp in artificial tear solution (pH 7.4) at 35°C, SDS (2%) was added to overcome the ITZ dissolubility problem and meet the sink conditions. The drug release from ITZ-M was characterized and compared to the drug suspension in terms of the release rate and extent, as shown in Figure 3. Approximately 59.90% of ITZ was released from the micelles within 96 h. For comparison, approximately 31.96% of ITZ was released from the suspension at the end time point. Moreover, both profiles fitted best to the Korsmeyer-Peppas equation, with R^2 values of 0.9888 and 0.9746 for ITZ-M and ITZ-Susp, respectively (Table 1). It is well known that the drug release from polymer micelles is a complicated process and influenced by several factors. According to the Korsmeyer-Peppas theory, if $n \leq 0.43$, drug release follows the Fickian diffusion mechanism, for $0.43 < n < 0.85$, non-Fickian diffusion; $n = 0.85$, the drug release follows case II transport; and $n > 0.85$, super-case II

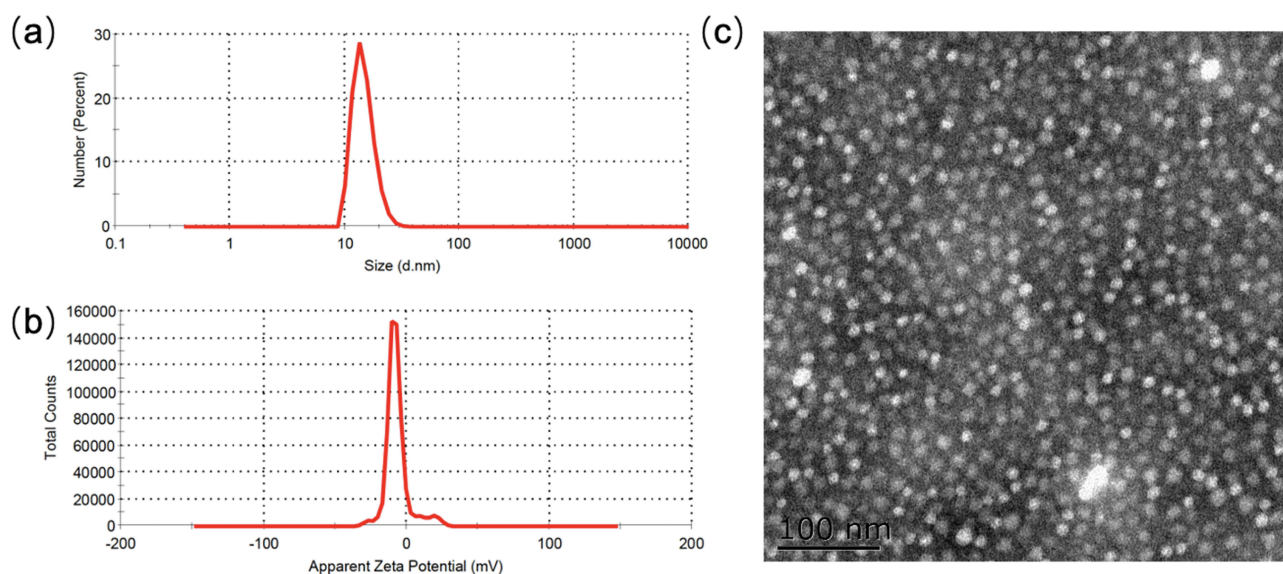


Figure 1 Characterization of ITZ-M. (a) droplet size distribution of ITZ-M; (b) zeta potential of ITZ-M; (c) TEM images of ITZ-M.

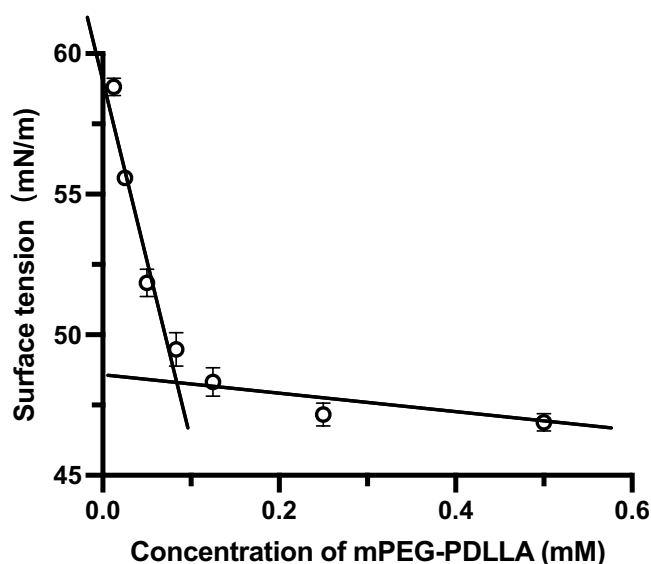


Figure 2 Surface tension versus concentration of mPEG-PDLLA.

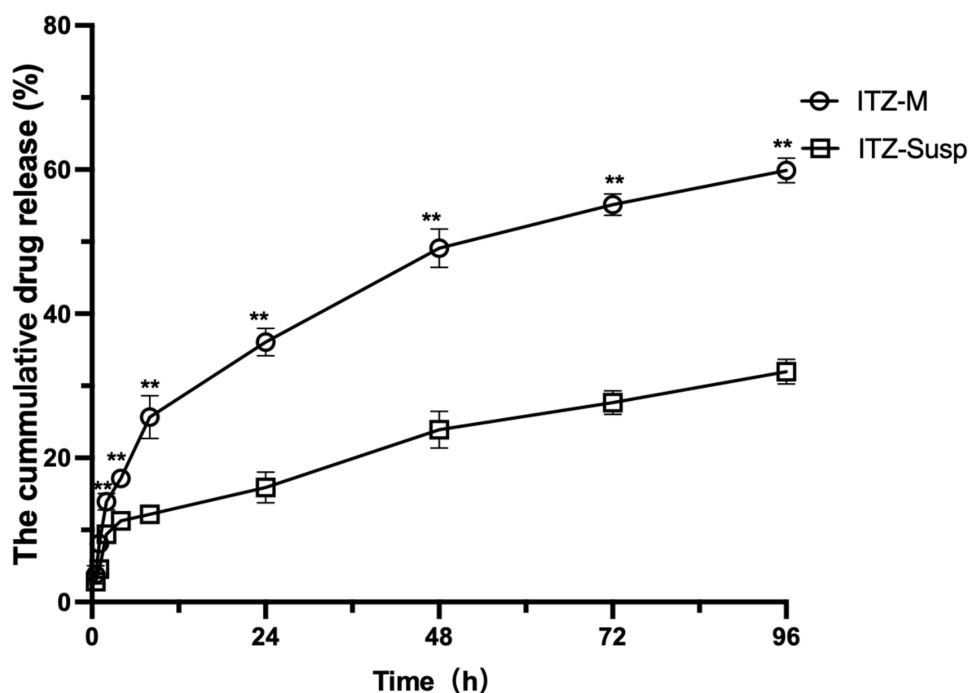


Figure 3 In vitro ITZ release profiles from ITZ-M and ITZ-Susp. Data represented as mean \pm SD, $n = 3$; all $**p < 0.01$, compared to ITZ-Susp.

transport.^{32,33} As shown in Table 1, the value of the release exponent “ n ” for ITZ-M was 0.397, indicating a Fickian release mechanism of ITZ-M in which drug release was controlled by diffusion.³²

Storage Stability

The formulation of ITZ-M did not precipitate or crystallize during the test period at 4°C, there were no significant changes occurring in DS, PDI, drug content, or EE%, as shown in Figure 4, which suggested that the ITZ-M was relatively stable at 4°C for 8 weeks. However, some drugs precipitated out at 25°C within one week. Micellization is entropically driven by hydrophobic effects. The aqueous molecules are expelled from the core of the forming micelle into the bulk water phase.³⁴

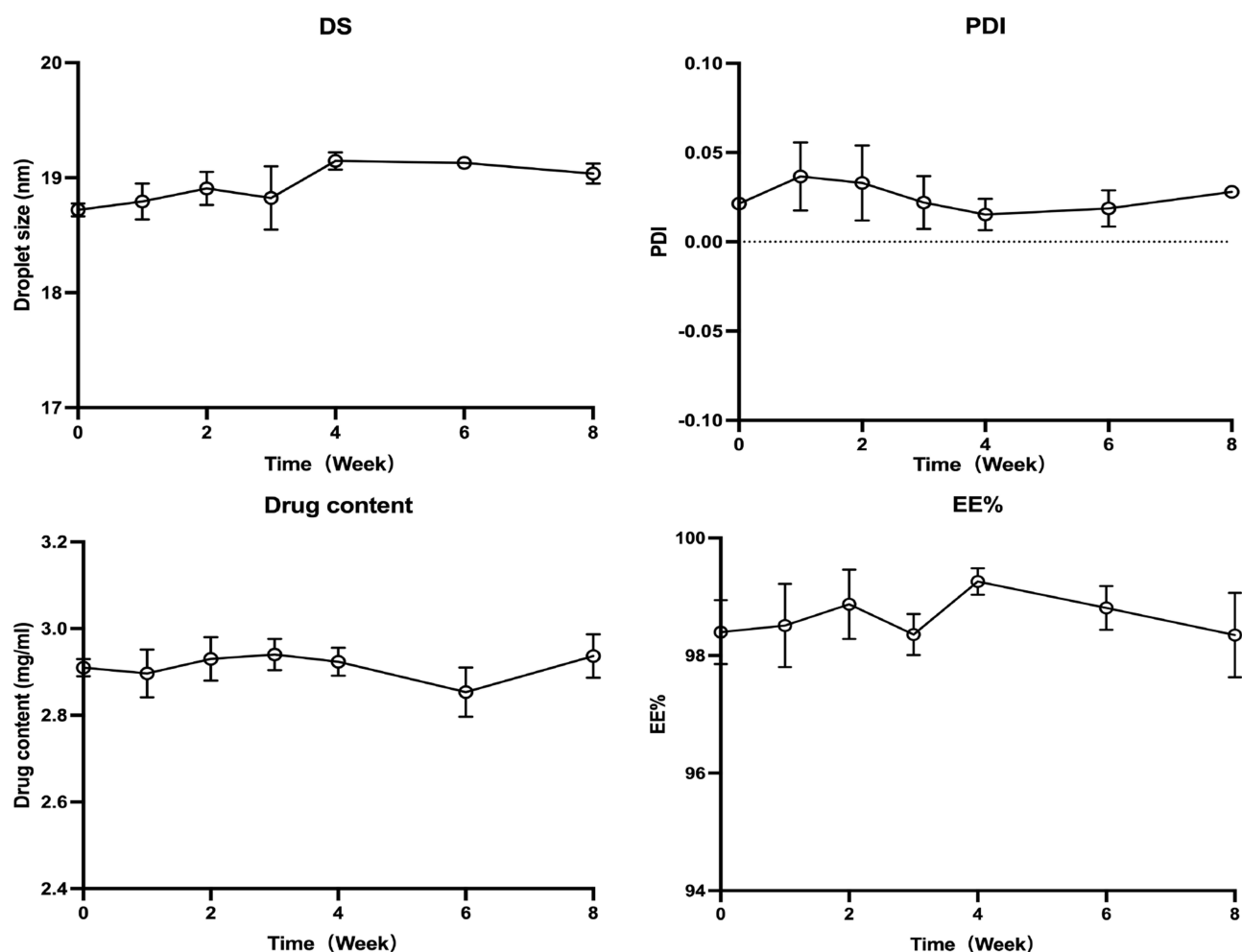
Table 1 The Squared Correlation Coefficients (R^2) and Equations for the Different Mathematical Models Fitted to the Release of ITZ

	ITZ-M		ITZ-Susp	
	Equation	R^2	Equation	R^2
Zero order	$Q = 0.5559 \times t + 14.09$	0.8677	$Q = 7.687 \times t + 0.276$	0.9109
First order	$Q = 54.54 \times (1 - e^{-0.069t})$	0.9349	$Q = 27.73 \times (1 - e^{-0.064t})$	0.8159
Higuchi	$Q = 6.05 \times t^{1/2} + 4.289$	0.9790	$Q = 2.934 \times t^{1/2} + 3.111$	0.9714
Korsmeyer-Peppas	$Q = 10.10 \times t^{0.397}$	0.9888	$Q = 5.523 \times t^{0.378}$	0.9746

Jule reported that an increase in the temperature was attributed to a higher mobility and greatly affected the inter-molecular distance between encapsulated molecule.³⁵ It has also been reported that the increase in temperature could significantly accelerated the chain exchange of mPEG-PDLLA and showed the importance of the core structure in the dynamic stability of the polymer micelles.³⁶ Thus, the stability data showed that the ITZ-M systems should be stored at 4°C.

Cytotoxicity

Cytotoxicity of the ITZ-M formulation was assessed using the CCK-8 assay. The viability of HCECs cell treated with ITZ at concentrations of 1.5, 0.3, 0.06 and 0.03 mg/mL after 15 min, 1h, 2h and 4h were shown in Figure 5. The results

**Figure 4** Changes in DS, PDI, drug content and EE% of ITZ-M at 4°C.

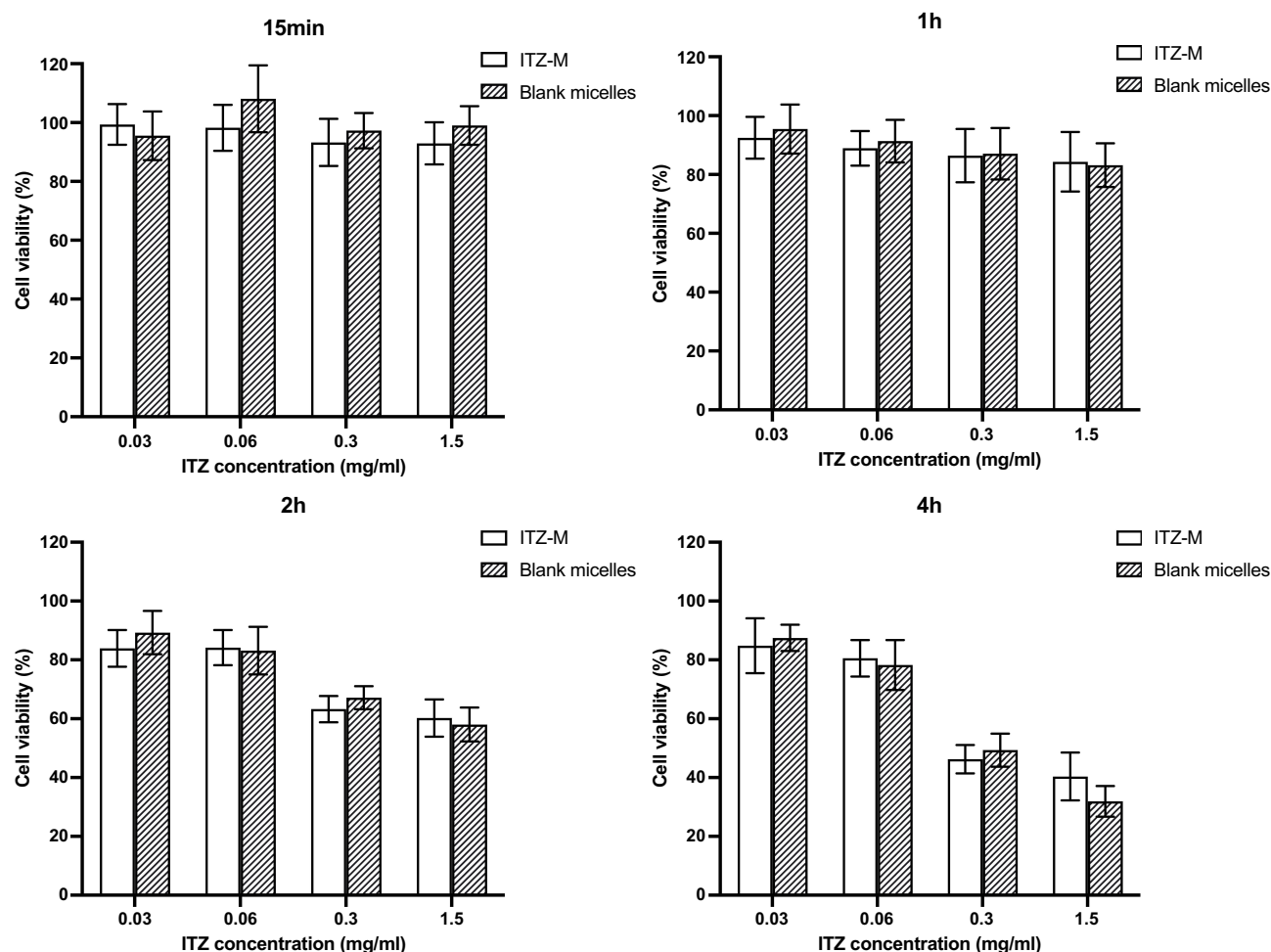


Figure 5 Cell viabilities of HCECs cultivated for 15 min, 1h, 2h and 4h after treating with a series of blank mPEG-PDLLA micelles and ITZ-M at different concentrations ($n = 5$).

indicated that the cell viability of HCECs were all more than 80% at the drug's concentrations of 0.03 and 0.06 mg/mL after treating for different times, which suggested that ITZ-M had no cytotoxicity at 0.03 and 0.06 mg/mL, while for ITZ-M at drug's levels of 0.3 and 1.5 mg/mL, the cell viability of HCECs decreased gradually with the cultivation time increasing. The cytotoxicity of ITZ-M was time- and concentration-dependent, it did not show any cytotoxicity effects on the HCECs at the concentrations of 0.06 mg/mL or lower.

In vitro Antifungal Activity

The inhibition zone's diameter for ITZ-M against *Aspergillus* was 17.7 ± 0.5 mm, while that for ITZ-Susp was not obtained treated at the same dose (Figure 6). The results of the antifungal activity study revealed that ITZ showed an improved antifungal effect when formulated in micellar form. Based on these data, it was suggested that the micellar structure increased the anti-fungal activity of ITZ. This effectiveness could be related to the increased aqueous solubility of ITZ by the micellar carriers. The increase in the solubility of the anti-fungal agent in water improved the effects of fungus inhibition in disc diffusion studies.³⁷ The antifungal activity observed in ITZ-M is entirely attributed to the increased aqueous solubility of ITZ. Blank micelles did not exhibit anti-fungal activity.

Corneal Permeation Studies

The corneal permeation behavior of mPEG-PDLLA micelles was observed using C6 as a poorly water-soluble model marker, as shown in Figure 7. The fluorescence signal was mostly enriched in the corneal epithelium, and the

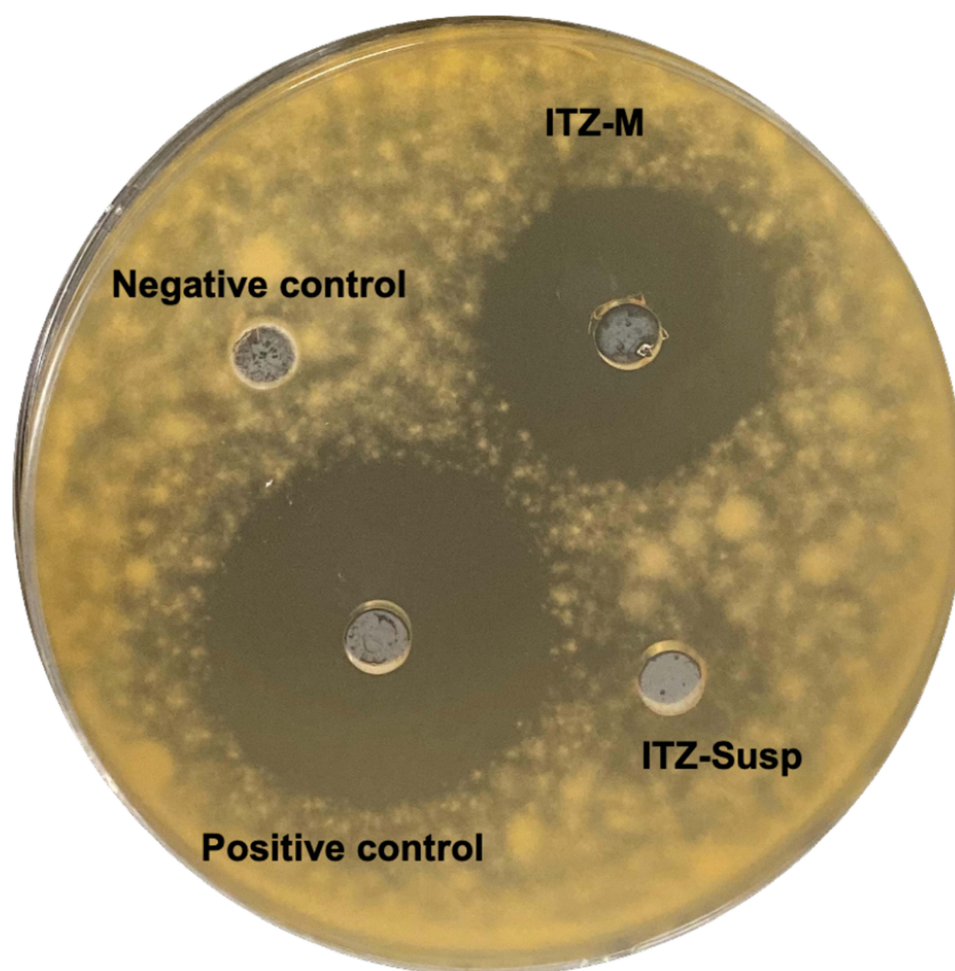


Figure 6 Antifungal activity of ITZ-M against *Aspergillus* using the agar plate diffusion method.

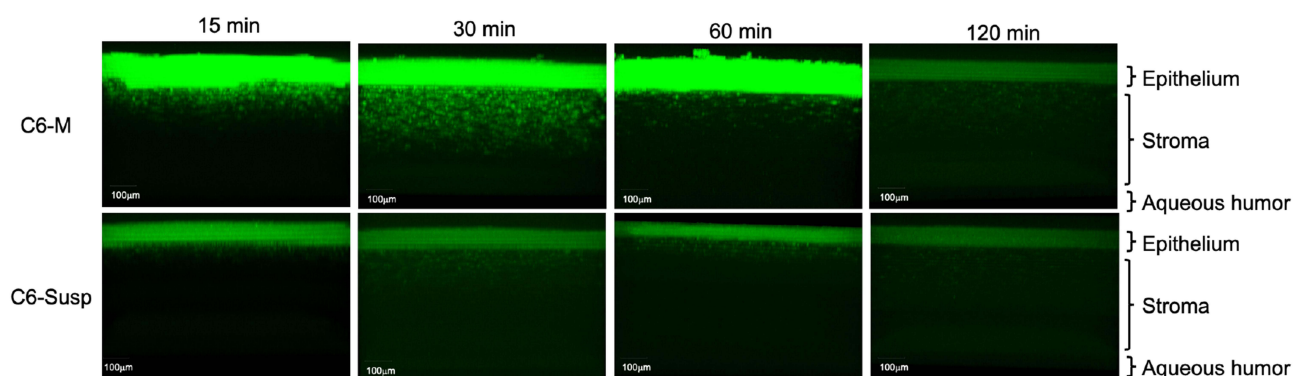


Figure 7 In vivo two-photon microscopy images of corneal cross-sections at 15, 30, 60 and 120 min after instilling the C6-M and C6-Susp formulations in rabbit eyes.

fluorescence intensity was reduced in the stroma. The fluorescence intensity increased in the stroma with time increasing at the first 30 min, after that, the fluorescence intensity decreased, and the fluorescence was nearly vanished after 120 min in the stroma. Compared with C6-Susp, more C6 could be delivered to the epithelium and stroma of the cornea by mPEG-PDLLA micelles, and micelles as nanosized carriers enhanced poorly soluble drug penetration into the cornea. This could be attributed to the following reasons: (1) the significant increase in the solubility of ITZ (from 4 ng/mL to 3 mg/mL), which enhanced its levels in the precorneal tear film and created a higher concentration gradient for the

barrier,³⁸ and (2) the nanometric size of the micelles (<20 nm) that facilitated their passage across the hydrated network of stroma of the cornea,³⁹ (3) in addition to paracellular routes, C6-M could also be transported across the corneal epithelium via transcellular routes because of increased uptake.^{40,41}

Ocular Irritation Test

As shown in Figure 8, after topical application of ITZ-M, the rabbit eyes showed no obvious ocular symptoms, such as congestion, edema, and discharge, in the cornea, conjunctiva, or iris during the test period. Moreover, according to the Draize test, the average total scores of the eyes treated with ITZ-M were less than 1 at all observed time points, suggesting that ITZ-M caused no significant irritation to the eyes. No fluorescence staining of the corneal epithelial layer was observed under cobalt blue light by slip-lamp microscopy at any time point, which indicated that ITZ-M did not cause significant damage to the corneal epithelial layer. In addition, Figure 9 showed the histopathology of the corneas and conjunctiva of the eyes 72 h after instilling the ITZ-M. It can be seen that the structure of the corneal epithelium layer was intact and normal, and there were no obvious defects or inflammatory cell infiltration in the cornea and conjunctiva. It can be concluded that the ITZ-M was safe for topical ocular application.

Ocular Pharmacokinetic Studies in Rabbit Eyes

The concentration–time curves of ITZ concentration in rabbit tears, corneas, and conjunctiva were shown in Figure 10 after topical administration of ITZ-M and ITZ-Susp. The pharmacokinetic parameters of the tear, corneal, and conjunctival tissues were listed in Table 2. The drug could be detected in the eyes treated with ITZ-M after 4 h in tear, corneal, and conjunctival tissues, whereas in the rabbit eyes treated with ITZ-Susp, the drug could be detected in the conjunctiva at all predetermined time points, but the drug in the tear and corneal tissues was undetectable after 30 min. In the first 30 min, the drug concentrations in the tear, cornea, and conjunctival tissues of rabbit eyes instilled with ITZ-M were significantly higher than those in rabbit eyes instilled with ITZ-Susp at 5, 15, and 30 min (all $p < 0.05$). The areas under the drug concentration curve ($AUC_{0-240\text{min}}$ ($\mu\text{g/g}\cdot\text{min}$)) for the tear, cornea and conjunctiva in rabbit eyes treated with ITZ-M were 6953.77, 1084.93 and 739.98 $\mu\text{g/g}\cdot\text{min}$, respectively, which were 52.8-, 410.96-, and 2.29-fold higher than those in the corresponding tissues in rabbit eyes treated with ITZ-Susp. The mean residence time ($MRT_{0-240\text{min}}$) of the drug in the tear, cornea, and conjunctiva in rabbit eyes treated with ITZ-M was 49.57, 73.86 and 84.77 min, and that in the conjunctiva treated with ITZ-Susp was 89.04 min. The results demonstrated that micelles, as ocular drug delivery systems, could increase the ocular bioavailability of ITZ compared to that of pure drugs.

The tear kinetics study demonstrated that the clearance of ITZ-Susp was significantly high, and the ITZ concentration rapidly declined in comparison to the same concentration of ITZ-M (Figure 10a). Furthermore, the decrease in tear ITZ

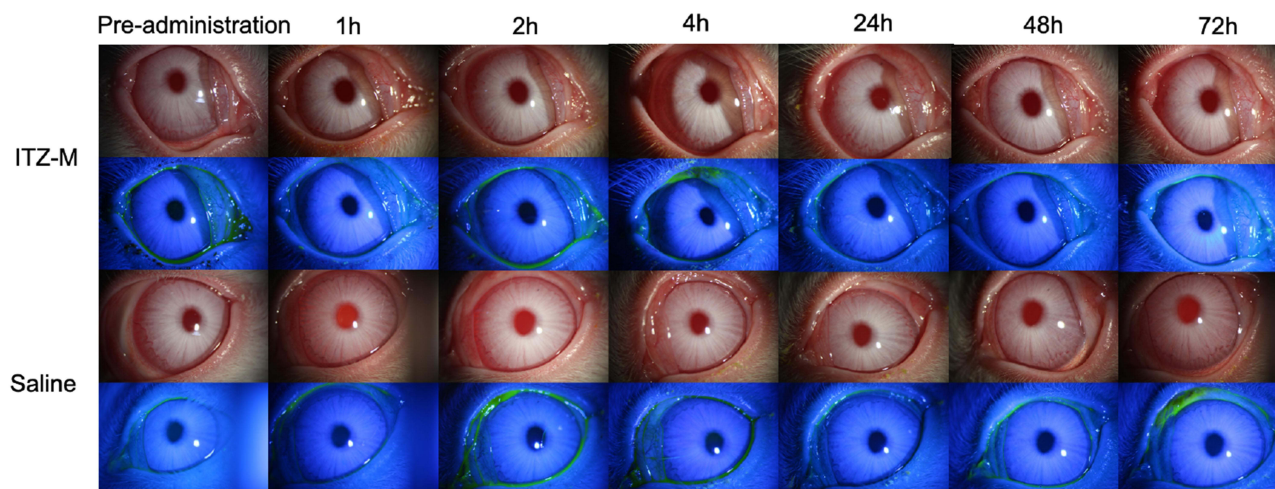


Figure 8 Visible light and Cobalt blue light photographs after loading dose (50 μL each time, once every five minutes for five times) of ITZ-M (right eye), saline served as control (left eye), at different times.

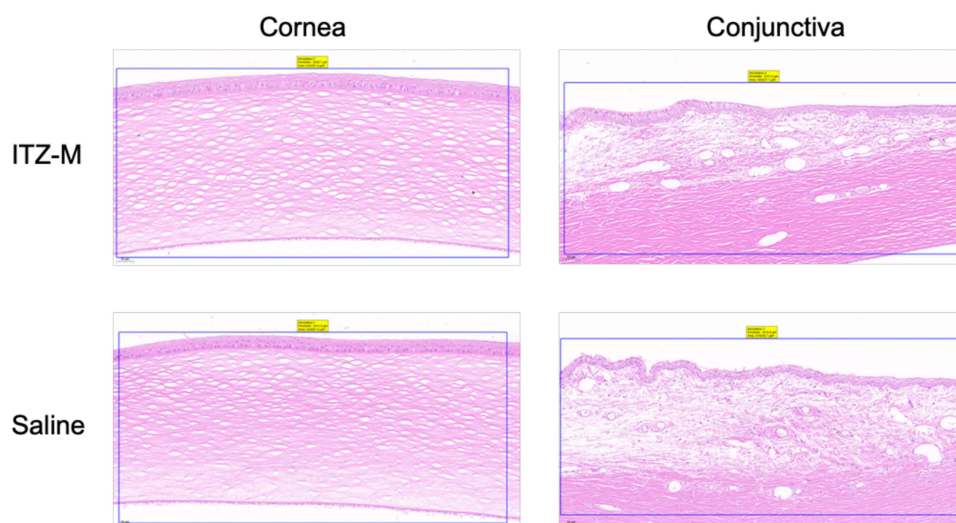


Figure 9 Histopathologic images of cornea and conjunctiva of rabbit eyes at 72 h after topical loading dose.

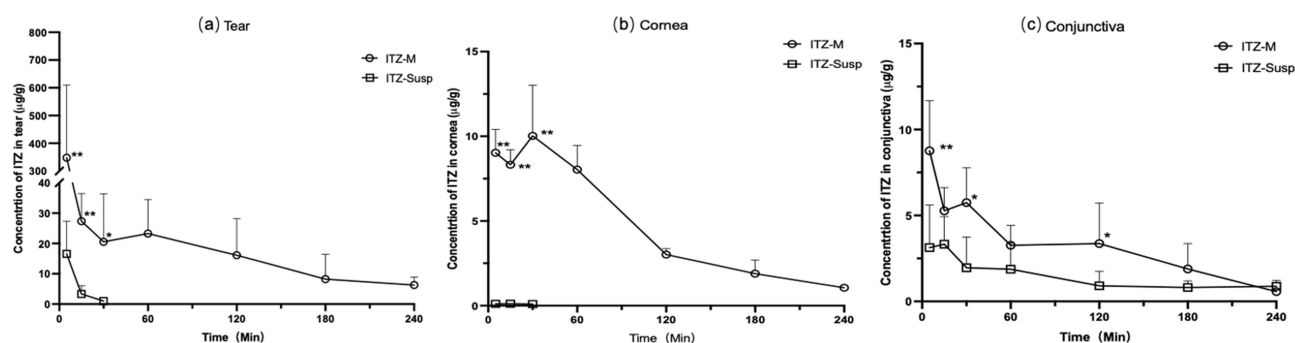


Figure 10 Concentration–time curves of ITZ in rabbit tear (a), cornea (b) and conjunctiva (c) after loading dose (50 μ L each time, once every five minutes for five times) of ITZ-M and ITZ-Susp. Data represented as mean \pm SD, $n = 6$; * $p < 0.05$, ** $p < 0.01$, compared to ITZ-Susp. (The drug levels in tear and cornea in ITZ-Susp group were under detection limit after 30 min).

concentration over time could be due to absorption across the cornea and conjunctiva (Figure 10b and c). In addition, previous studies have shown that prolonging the residence time in the precorneal region could improve the penetration of drug across cornea.^{42–44} The improvement which could be attributed to the interaction of the PEG tail on the surface of ITZ-M, which interacts with mucin and improves the residence time over the cornea.^{42,45}

Table 2 Pharmacokinetic Parameters of ITZ in Rabbit Eyes Following Loading Dose (50 μ L Each Time, Once Every Five minutes for Five Times) Topical Application of ITZ-M and ITZ-Susp

Tissue	Drug	Pharmacokinetic Parameters				
		C_{\max} (μ g/g)	T_{\max} (min)	$t_{1/2}$ (min)	$AUC_{(0-240\text{min})}$ (μ g/g min)	$MRT_{(0-240\text{min})}$ (min)
Tear	ITZ-M	348.11 ± 261.89	5	94.13	6953.77	49.57
	ITZ-Susp	16.55 ± 10.73	5	/	131.7	/
Cornea	ITZ-M	10.02 ± 3.00	30	64.30	1084.93	73.86
	ITZ-Susp	0.11 ± 0.04	15	/	2.64	/
Conjunctiva	ITZ-M	8.76 ± 2.92	5	65.71	739.98	84.77
	ITZ-Susp	3.33 ± 1.62	15	176.43	322.8	89.04

According to the calculated $AUC_{(0-240\text{min})}$ values, the increase in corneal and conjunctival bioavailability for ITZ-M was 410.96 and 2.29 fold higher than the same dose of ITZ-Susp in the corresponding tissues, respectively. The increase in drug penetration across the cornea and conjunctiva following the instillation of ITZ-M could be related to the colloidal carrier nature of nanoparticles and the appropriate drug lipophilicity.⁴⁶ It has been reported that the ideal lipophilicity for transcorneal drug delivery could be a log P value of 2–3.⁴⁷ With a log P value of 7.13⁴⁸ and extremely low water solubility (approximately 4 ng/mL),^{12,13} it resulted in poor corneal and conjunctival penetration. This is similar to the results of vision corneal permeation studies using in vivo two-photon microscopy. Nanometer-sized particles (presently 18 nm) could provide better bioadhesion and greater surface area for interaction with the cornea and conjunctiva.^{49,50} They could also pass through the ocular biological membrane barriers and enhance penetration through the cornea.^{51,52} Nanocarriers could prolong the retention time in the precorneal area of the eye because of their size and ability to adhere to the ocular surface.^{42,43} Furthermore, the interaction of micelles with the glycoproteins of the cornea and conjunctiva could form a precorneal depot to prolong the release of micelles loaded with the drug. It has been reported that the values of minimal inhibitory concentration for 90% of the strains (MIC_{90}) against *Aspergillus (A.) flavus*, *A. fumigatus* and *A. niger* isolated from human keratomycosis patients, the main pathogenic fungus for the fungal corneal ulcers, were 0.25–1 $\mu\text{g/mL}$, 0.125–1 $\mu\text{g/mL}$ and 0.25–0.5 $\mu\text{g/mL}$, respectively.^{53,54} The ITZ concentrations in the cornea after loading dose application of ITZ-M were all above the MIC_{90} against the three isolates of *Aspergillus* during the determined time period, indicating that another administration is not necessary for at least four hours. Nevertheless, the corneal drug concentrations of ITZ from ITZ-Susp after loading dose administration were lower than the MIC_{90} , indicating that ITZ-Susp were not effective when applied topically. Therefore, ITZ-M shows a significant advantage in terms of topical administration.

Conclusions

A topically applied ophthalmic micelle solution containing ITZ was successfully prepared based on mPEG-PDLLA, using the thin-film dispersion method. The ITZ-loaded mPEG-PDLLA micelles exhibited adequately small particle size, narrow size distribution, good physical stability, and high entrapment efficiency. ITZ-M showed a rapid in vitro drug release rate and extent compared with the drug suspension. The ITZ-M demonstrated good tolerance and safety. In addition, ITZ-M also enhanced in vitro antifungal activity and improved corneal permeability compared to ITZ-Susp. In vivo ocular pharmacokinetic studies in rabbits showed that ITZ-M increased the concentrations of ITZ in tear, corneal, and conjunctival tissues, demonstrating that ITZ-M had higher ocular bioavailability than ITZ-Susp. In conclusion, ITZ-M may be a potential ocular drug delivery system and prospective treatment strategy for FK.

Abbreviations

ITZ, itraconazole; mPEG-PDLLA, methoxy poly(ethylene glycol)-poly(D, L-lactic acid); ITZ-M, ITZ loaded mPEG-PDLLA micelles; DS, droplet size; ZP, zeta potential; PDI, polydispersity index; EE%, entrapment efficiency; CMC, critical micelle concentration; HCECs, human corneal epithelial cells; C6-M, micelles labeled with coumarin 6; FI, fluorescence intensity; $AUC_{0-240\text{min}}$, the area under the curve up to 240 min; FK, fungal keratitis; DMEM, dulbecco's modified eagle medium; ITZ-Susp, ITZ suspension; HPLC, high performance liquid chromatography; TEM, transmission electron microscopy; CCK-8, cell counting kit-8; OD, optical density; C6-Susp, C6 suspension; H&E, hematoxylin and eosin; AH, aqueous humor; SD, standard deviation; $MRT_{0-240\text{min}}$, mean residence time up to 240 min; MIC_{90} , minimal inhibitory concentration for 90% of the strains; C_{max} , the maximum concentration; T_{max} , the time for C_{max} to occur; $t_{1/2}$, the elimination half-life time.

Ethics Approval and Informed Consent

This study was approved by the Laboratory Animal Ethics Committee of the Henan Provincial Eye Institute (approval number: HNEECA-2022-32). All procedures involving animals were performed in accordance with the guidelines of the National Institutes of Health and the Association for Research in Vision and Ophthalmology Resolution.

Author Contributions

All authors made a significant contribution to the work reported, whether that is in the conception, study design, execution, acquisition of data, analysis and interpretation, or in all these areas; took part in drafting, revising or critically reviewing the article; gave final approval of the version to be published; have agreed on the journal to which the article has been submitted; and agree to be accountable for all aspects of the work.

Disclosure

The authors declare no conflicts of interest in this work.

References

- Mascarenhas M, Chaudhari P, Lewis SA. Natamycin ocular delivery: challenges and advancements in ocular therapeutics. *Adv Ther.* 2023;40(8):3332–3359. doi:10.1007/s12325-023-02541-x
- Awad R, Ghaith AA, Awad K, Mamdouh Saad M, Elmassry AA. Fungal keratitis: diagnosis, management, and recent advances. *Clin Ophthalmol.* 2024;18:85–106. doi:10.2147/OPTH.S447138
- Bisen AC, Sanap SN, Agrawal S, et al. Etiopathology, epidemiology, diagnosis, and treatment of fungal keratitis. *ACS Infect Dis.* 2024;10(7):2356–2380. doi:10.1021/acsinfecdis.4c00203
- Tena D, Rodriguez N, Toribio L, Gonzalez-Praetorius A. Infectious keratitis: microbiological review of 297 cases. *Jpn J Infect Dis.* 2019;72(2):121–123. doi:10.7883/yoken.JJID.2018.269
- Mittal R, Ahooja H, Sapra N. Corneal “Plaque” formation after anti-acanthamoeba therapy in acanthamoeba keratitis. *Indian J Ophthalmol.* 2018;66(11):1623–1624. doi:10.4103/ijo.IJO_734_18
- Castano G, Elnahry AG, Mada PK. Fungal keratitis. In: *StatPearls*. StatPearls Publishing; 2025.
- Hoffman JJ, Burton MJ, Leck A. Mycotic keratitis—a global threat from the filamentous fungi. *J Fungi.* 2021;7(4):273. doi:10.3390/jof7040273
- Qiu S, Zhao GQ, Lin J, et al. Natamycin in the treatment of fungal keratitis: a systematic review and meta-analysis. *Int J Ophthalmol.* 2015;8(3):597–602. doi:10.3980/j.issn.2222-3959.2015.03.29
- FlorCruz NV, Evans JR. Medical interventions for fungal keratitis. *Cochrane Database Syst Rev.* 2015;2015(4):CD004241. doi:10.1002/14651858.CD004241.pub4
- Saag MS, Dismukes WE. Azole antifungal agents: emphasis on new triazoles. *Antimicrob Agents Chemother.* 1988;32(1):1–8. doi:10.1128/AAC.32.1.1
- Mohanty B, Majumdar DK, Mishra SK, Panda AK, Patnaik S. Development and characterization of itraconazole-loaded solid lipid nanoparticles for ocular delivery. *Pharm Dev Technol.* 2015;20(4):458–464. doi:10.3109/10837450.2014.882935
- Parikh T, Sandhu HK, Talele TT, Serajuddin AT. Characterization of solid dispersion of itraconazole prepared by solubilization in concentrated aqueous solutions of weak organic acids and drying. *Pharm Res.* 2016;33(6):1456–1471. doi:10.1007/s11095-016-1890-8
- Sayed S, Elsayed I, Ismail MM. Optimization of beta-cyclodextrin consolidated micellar dispersion for promoting the transcorneal permeation of a practically insoluble drug. *Int J Pharm.* 2018;549(1–2):249–260. doi:10.1016/j.ijpharm.2018.08.001
- Rajasekaran J, Thomas PA, Kalavathy CM, Joseph PC, Abraham DJ. Itraconazole therapy for fungal keratitis. *Indian J Ophthalmol.* 1987;35(5–6):157–160.
- Thomas PA, Rajasekaran J. Treatment of aspergillus keratitis with imidazoles and related compounds. In: *Aspergillus and aspergillosis*. Boston, MA: Springer US; 1988:267–279.
- Klippenstein K, O'Day DM, Robinson RD, Williams TE, Head WS. The qualitative evaluation of the pharmacokinetics of subconjunctivally injected antifungal agents in rabbits. *Cornea.* 1993;12(6):512–516. doi:10.1097/00003226-199311000-00009
- Friedberg ML, Pleyer U, Mondino BJ. Device drug delivery to the eye. Collagen shields, iontophoresis, and pumps. *Ophthalmology.* 1991;98(5):725–732. doi:10.1016/s0161-6420(91)32227-9
- Shi L, Li Z, Liang Z, et al. A dual-functional chitosan derivative platform for fungal keratitis. *Carbohydr Polym.* 2022;275:118762. doi:10.1016/j.carbpol.2021.118762
- Guo Z, Shi L, Feng H, et al. Reduction-sensitive nanomicelles: delivery celastrol for retinoblastoma cells effective apoptosis. *Chin Chem Lett.* 2021;32(3):1046–1050. doi:10.1016/j.cclet.2020.03.066
- Li J, Li Z, Liang Z, et al. Fabrication of a drug delivery system that enhances antifungal drug corneal penetration. *Drug Deliv.* 2018;25(1):938–949. doi:10.1080/10717544.2018.1461278
- Zhang X, Wu Y, Zhang M, et al. Sodium cholate-enhanced polymeric micelle system for tumor-targeting delivery of paclitaxel. *Int J Nanomed.* 2017;12:8779–8799. doi:10.2147/IJN.S150196
- Younis MA, Tawfeek HM, Abdellatif AAH, Abdel-Aleem JA, Harashima H. Clinical translation of nanomedicines: challenges, opportunities, and keys. *Adv Drug Deliv Rev.* 2022;181:114083. doi:10.1016/j.addr.2021.114083
- Xu M, Yao C, Zhang W, Gao S, Zou H, Gao J. Anti-cancer activity based on the high docetaxel loaded Poly(2-Oxazoline)s micelles. *Int J Nanomed.* 2021;16:2735–2749. doi:10.2147/IJN.S298093
- Jo MJ, Lee YJ, Park CW, et al. Evaluation of the physicochemical properties, pharmacokinetics, and in vitro anticancer effects of docetaxel and osthonol encapsulated in methoxy Poly(ethylene glycol)-b-Poly(caprolactone) polymeric micelles. *Int J Mol Sci.* 2020;22(1):231. doi:10.3390/ijms22010231
- Jo MJ, Jo YH, Lee YJ, et al. Physicochemical, pharmacokinetic, and toxicity evaluation of methoxy Poly(ethylene glycol)-b-Poly(d,l-Lactide) polymeric micelles encapsulating alpinumisoflavone extracted from unripe cudrania tricuspidata fruit. *Pharmaceutics.* 2019;11(8):366. doi:10.3390/pharmaceutics11080366
- Su Y, Wang K, Li Y, et al. Sorafenib-loaded polymeric micelles as passive targeting therapeutic agents for hepatocellular carcinoma therapy. *Nanomedicine.* 2018;13(9):1009–1023. doi:10.2217/nnm-2018-0046
- Yu YL, Li YN, Zhang Y, Sun RN, Tu JS, Shen Y. Optimization and characterization of deoxypodophyllotoxin loaded mPEG-PDLLA micelles by central composite design with response surface methodology. *Chin J Nat Med.* 2018;16(6):471–480. doi:10.1016/S1875-5364(18)30081-5

28. Zhang Y, Wang S, Duan X, et al. mPEG-PDLLA micelles potentiate docetaxel for intraperitoneal chemotherapy in ovarian cancer peritoneal metastasis. *Front Pharmacol.* **2022**;13:861938. doi:10.3389/fphar.2022.861938
29. He H, Wang L, Ma Y, et al. The biological fate of orally administered mPEG-PDLLA polymeric micelles. *J Control Release.* **2020**;327:725–736. doi:10.1016/j.jconrel.2020.09.024
30. Moazeni E, Gilani K, Najafabadi AR, et al. Preparation and evaluation of inhalable itraconazole chitosan based polymeric micelles. *DARU J Pharma Sci.* **2012**;20(1):85. doi:10.1186/2008-2231-20-85
31. Lu P, Liang Z, Zhang Z, et al. Novel nanomicelle butenafine formulation for ocular drug delivery against fungal keratitis: in vitro and in vivo study. *Eur J Pharm Sci.* **2024**;192:106629. doi:10.1016/j.ejps.2023.106629
32. Kassem AA, Abd El-Alim SH, Basha M, Salama A. Phospholipid complex enriched micelles: a novel drug delivery approach for promoting the antidiabetic effect of repaglinide. *Eur J Pharm Sci.* **2017**;99:75–84. doi:10.1016/j.ejps.2016.12.005
33. Usman F, Farooq M, Wani TA, et al. Itraconazole loaded biosurfactin micelles with enhanced antifungal activity: fabrication, evaluation and molecular simulation. *Antibiotics.* **2023**;12(10):1550. doi:10.3390/antibiotics12101550
34. Croy SR, Kwon GS. Polymeric micelles for drug delivery. *Curr Pharm Des.* **2006**;12(36):4669–4684. doi:10.2174/138161206779026245
35. Jule E, Yamamoto Y, Thouvenin M, Nagasaki Y, Kataoka K. Thermal characterization of poly(ethylene glycol)-poly(D,L-lactide) block copolymer micelles based on pyrene excimer formation. *J Control Release.* **2004**;97(3):407–419. doi:10.1016/j.jconrel.2004.02.012
36. Yamamoto Y, Yasugi K, Harada A, Nagasaki Y, Kataoka K. Temperature-related change in the properties relevant to drug delivery of poly(ethylene glycol)-poly(D,L-lactide) block copolymer micelles in aqueous milieu. *J Control Release.* **2002**;82(2–3):359–371. doi:10.1016/s0168-3659(02)00147-5
37. Durgun ME, Kahraman E, Hacioglu M, Gungor S, Ozsoy Y. Posaconazole micelles for ocular delivery: in vitro permeation, ocular irritation and antifungal activity studies. *Drug Deliv Transl Res.* **2022**;12(3):662–675. doi:10.1007/s13346-021-00974-x
38. Noh G, Keum T, Seo JE, et al. Development and evaluation of a water soluble fluorometholone eye drop formulation employing polymeric micelle. *Pharmaceutics.* **2018**;10(4):208. doi:10.3390/pharmaceutics10040208
39. Zhou T, Zhu L, Xia H, et al. Micelle carriers based on macrogol 15 hydroxystearate for ocular delivery of terbinafine hydrochloride: in vitro characterization and in vivo permeation. *Eur J Pharm Sci.* **2017**;109:288–296. doi:10.1016/j.ejps.2017.08.020
40. Liu C, Lan Q, He W, et al. Octa-arginine modified lipid emulsions as a potential ocular delivery system for disulfiram: a study of the corneal permeation, transcorneal mechanism and anti-cataract effect. *Colloids Surf B Biointerfaces.* **2017**;160:305–314. doi:10.1016/j.colsurfb.2017.08.037
41. Salama AH, Shamma RN. Tri/tetra-block co-polymeric nanocarriers as a potential ocular delivery system of lornoxicam: in-vitro characterization, and in-vivo estimation of corneal permeation. *Int J Pharm.* **2015**;492(1–2):28–39. doi:10.1016/j.ijpharm.2015.07.010
42. Sathe P, Kailasam V, Nagarjuna V, et al. Nanomicelles empower natamycin in treating fungal keratitis: an in vitro, ex vivo and in vivo study. *Int J Pharm.* **2024**;656:124118. doi:10.1016/j.ijpharm.2024.124118
43. Chandasana H, Prasad YD, Chhonker YS, et al. Corneal targeted nanoparticles for sustained natamycin delivery and their PK/PD indices: an approach to reduce dose and dosing frequency. *Int J Pharm.* **2014**;477(1–2):317–325. doi:10.1016/j.ijpharm.2014.10.035
44. Cholkar K, Gunda S, Earla R, Pal D, Mitra AK. Nanomicellar topical aqueous drop formulation of rapamycin for back-of-the-eye delivery. *AAPS Pharm Sci Tech.* **2015**;16(3):610–622. doi:10.1208/s12249-014-0244-2
45. Huckaby JT, Lai SK. PEGylation for enhancing nanoparticle diffusion in mucus. *Adv Drug Deliv Rev.* **2018**;124:125–139. doi:10.1016/j.addr.2017.08.010
46. Tayel SA, El-Nabarawi MA, Tadros MI, Abd-Elsalam WH. Positively charged polymeric nanoparticle reservoirs of terbinafine hydrochloride: preclinical implications for controlled drug delivery in the aqueous humor of rabbits. *AAPS Pharm Sci Tech.* **2013**;14(2):782–793. doi:10.1208/s12249-013-9964-y
47. Mannermaa E, Vellonen KS, Urtti A. Drug transport in corneal epithelium and blood-retina barrier: emerging role of transporters in ocular pharmacokinetics. *Adv Drug Deliv Rev.* **2006**;58(11):1136–1163. doi:10.1016/j.addr.2006.07.024
48. Riccardi K, Cawley S, Yates PD, et al. Plasma protein binding of challenging compounds. *J Pharm Sci.* **2015**;104(8):2627–2636. doi:10.1002/jps.24506
49. Kakkar S, Karuppaiyl SM, Raut JS, et al. Lipid-polyethylene glycol based nano-ocular formulation of ketoconazole. *Int J Pharm.* **2015**;495(1):276–289. doi:10.1016/j.ijpharm.2015.08.088
50. Yoncheva K, Lizarraga E, Irache JM. Pegylated nanoparticles based on poly(methyl vinyl ether-co-maleic anhydride): preparation and evaluation of their bioadhesive properties. *Eur J Pharm Sci.* **2005**;24(5):411–419. doi:10.1016/j.ejps.2004.12.002
51. Liang Z, Zhang Z, Yang J, et al. Assessment to the antifungal effects in vitro and the ocular pharmacokinetics of solid-lipid nanoparticle in rabbits. *Int J Nanomed.* **2021**;16:7847–7857. doi:10.2147/IJN.S340068
52. Nagarwal RC, Kant S, Singh PN, Maiti P, Pandit JK. Polymeric nanoparticulate system: a potential approach for ocular drug delivery. *J Control Release.* **2009**;136(1):2–13. doi:10.1016/j.jconrel.2008.12.018
53. Hassan AS, Sangeetha AB, Shobana CS, et al. In-vitro assessment of first-line antifungal drugs against *Aspergillus* spp. caused human keratomycoses. *J Infect Public Health.* **2020**;13(12):1907–1911. doi:10.1016/j.jiph.2020.10.014
54. Vanathi M, Naik R, Sidhu N, Ahmed NH, Gupta N, Tandon R. Evaluation of antifungal susceptibility and clinical characteristics in fungal keratitis in a tertiary care center in North India. *Indian J Ophthalmol.* **2022**;70(12):4270–4283. doi:10.4103/ijo.IJO_855_22